Consistent assignment of the vibrations of symmetric and asymmetric *meta*-disubstituted benzenes

David J. Kemp, William D. Tuttle, Florence M. S. Jones, Adrian M. Gardner, Anna Andrejeva, Jonathan C. A. Wakefield and Timothy G. Wright[a,*]

[a]School of Chemistry, University of Nottingham, University Park, Nottingham, NG7 2RD, U.K.

*To whom correspondence should be addressed. Email: Tim.Wright@nottingham.ac.uk

Abstract

The assignment of vibrational structure in spectra gives valuable insights into geometric and electronic structure changes upon electronic excitation or ionization; particularly when such information is available for families of molecules. We give a description of the phenyl-ring-localized vibrational modes of the ground (S_0) electronic states of sets of *meta*-disubstituted benzene molecules including both symmetrically- and asymmetrically-substituted cases. As in our earlier work on monosubstituted benzenes [A. M. Gardner and T. G. Wright. J. Chem. Phys. 135 (2011) 114305], *para*-disubstituted benzenes [A. Andrejeva, A. M. Gardner, W. D. Tuttle, and T. G. Wright, J. Molec. Spectrosc. 321 (2016) 28], and *ortho*-disubstituted benzenes [W. D. Tuttle, A. M. Gardner, A. Andrejeva, D. J. Kemp, J. C. A. Wakefield and T. G. Wright, J. Molec. Spectrosc. 344 (2018) 46], we conclude that the use of the commonly-used Wilson or Varsányi mode labels, which are based on the vibrational motions of benzene itself, is misleading and ambiguous. Instead, we label the phenyl-ring-localized modes consistently based upon the Mulliken (Herzberg) method for the modes of *meta*-difluorobenzene (*m*DFB) under C_s symmetry, since we wish the labelling scheme to cover both symmetrically- and asymmetrically-substituted molecules. By studying the vibrational wavenumbers obtained from the same force-field while varying the mass of the substituent, we are able to follow the evolving modes across a wide range of molecules and hence provide consistent assignments. We assign the vibrations of the following sets of molecules: the symmetric *meta*-dihalobenzenes, *meta*-xylene and resorcinol (*meta*-dihydroxybenzene); and the asymmetric *meta*-dihalobenzenes, *meta*-halotoluenes, *meta*-halophenols and *meta*-cresol. In the symmetrically-substituted species, we find two pairs of in-phase and out-of-phase carbon-substituent stretches, and this motion persists in asymmetrically-substituted molecules for heavier substituents; however, when at least one of the substituents is light, then we find that these evolve into localized carbon-substituent stretches.

Keywords: Vibrations; Frequencies; Ground electronic state; *meta*-Disubstituted Benzenes

1. Introduction

Vibrations are key quantities by which spectroscopists gain insight into both geometric and electronic structures of molecules. Analyzing the vibrational activity during electronic transitions or ionization allows elucidation of resultant changes in geometry and, by looking at the changes in vibrational wavenumber, information on changes in electronic structure can be inferred. For reliable comparison between like-families of molecules one desires the consistent assignment of the spectral lines, in terms of the normal modes of the molecules. Problems arise in these comparisons as even quite small changes in structure can lead to significant changes in the appearance of the spectrum. These changes may be due to a change in the symmetry point group of the molecule, shifts in vibrational wavenumber as a result of mass differences, and electronic effects.

In the present and related work, we have focused particularly on the study of substituted benzenes, where comparison between molecules has often been obfuscated through the use of three different vibrational labelling schemes: the Wilson mode labels [1]; the related Varsányi [2] scheme; and the “Mulliken” [3] (or “Herzberg”) labels [4].We have previously discussed these schemes in great detail for monosubstituted benzenes [5], and concluded these were unreliable. Our solution to these problems is highlighted in detail in Ref. [5] for the case of monosubstituted benzenes. It comprised the use of quantum chemical calculations to calculate the force field of benzene and then to artificially increase the mass of a single hydrogen atom stepwise. We found that the variations in wavenumber appeared largely to settle down when the substituent mass reached approximately 15 amu, and only small changes in wavenumber were observed for any vibration above this. This then allowed fluorobenzene to be chosen as a sensible basis for the labelling (a substituent of 19 amu). A notable aspect is that changes in vibrational wavenumbers were apparently not significantly dependent on electronic effects (resonance or inductive).

In a similar way, the vibrational character is expected to change for disubstitutions, which can be viewed as a disubstitution of benzene, or a further substitution of a monosubstituted benzene. In order to have consistent labelling of vibrational motions we have found that it is required to have separate labelling schemes for monosubstituted [5], and *para*- [6] and *ortho*-disubstituted [7] benzenes. There is a degree of inconvenience in using multiple labelling schemes depending on the benzene isomer; however, this emphasises the point that assuming

vibrations of different substituted benzenes are the same, as implied by Wilson or Varsányi labels, is misleading.

The labelling scheme for the monosubstituted benzenes has been applied in a series of papers on vibrationally-resolved electronic spectra of jet-cooled monohalobenzenes – see Refs. [8], [9] and [10] – as well as in studies of toluene [11, 12] using zero-kinetic-energy (ZEKE) spectroscopy and two-dimensional laser induced fluorescence [13]; similarly, we have applied the scheme for *para*-disubstituted benzenes, which can be either symmetrically or asymmetrically disubstituted, in analyzing the vibrational activity following either electronic excitation or ionization in *para*-fluorotoluene (*p*FT) [14,15], *para*-xylene (*p*Xyl) [16,17], and *para*-chlorofluorobenzene (*p*ClFB) [18]. Through the use of these schemes we have been able to show clearly the high correspondence in vibrational activity between the aforementioned molecules.

Herein, we shall complete our examination of the vibrations of the S_0 states of disubstituted benzenes by considering different *meta*-disubstituted benzenes. We shall again conclude that it is not possible to use the Wilson (or Varsányi) labels, nor the Mulliken (or Herzberg) labels consistently. Furthermore, we will conclude that it is not possible to use the monosubstituted, *para*- nor *ortho*-disubstituted schemes for *meta*-disubstituted benzenes. We put forward a new labelling scheme to be used exclusively for *meta*-disubstituted benzenes, covering both the symmetrically- and asymmetrically-disubstituted molecules. We employ a scheme based upon the lowest common point group shared by the disubstituted benzene family which, in this case, is C_s symmetry, and base it on the vibrations of *meta*-difluorobenzene (*m*DFB).

2. Computational Details

All harmonic vibrational frequencies were obtained using B3LYP/aug-cc-pVTZ calculations via the GAUSSIAN 09 software package [19]. For bromine and iodine atoms, the full relativistic effective core potentials, ECP10MDF and ECP28MDF respectively, were used with corresponding aug-cc-pVTZ-PP valence basis sets. All calculated harmonic vibrational wavenumbers were scaled by a factor of 0.97 to account for anharmonicity and other deficiencies in the calculations. This level of calculation has been shown to be very reliable for the S_0 vibrational wavenumbers of a range of substituted benzenes. In the following, we shall calculate vibrational wavenumbers for the actual molecule, but also vibrational wavenumbers that are calculated using the force field of one molecule, but then artificially changing the mass of one or two atoms to match those of particular substituents (atomic or otherwise). In this way,

we are able to map out changes in the vibrational wavenumbers that occur solely from the mass effect and so identify any deviations from these. In addition, we shall calculate generalized Duschinsky matrices using FC-LabII [20] to illustrate the expression of the vibrations of one molecule in terms of another. For each molecule, we show results for a specific conformer, which will be the lowest energy one that we found at the indicated level of theory.

3. Labelling the S_0 vibrational modes of *m*DFB

We have previously described our methodology in great detail in Refs. [5 and 6]. We will thus present our results, only including previous detail when necessary for clarity.

We begin first by comparing the vibrations of *m*DFB with those of benzene. Similar to the situation in Ref. [7], a choice must be made about the axis system to be used. For ease of comparison we require the atoms in the molecule to be aligned in a way that each atom of the first molecule must appear superimposed on an atom of the second molecule. We therefore choose to place both *m*DFB and benzene in the *yz* plane with the *z* axis passing through a C-H bond, and we select the one that is located between the C-F bonds for *m*DFB – see Fig. 1.

Figure 1 represents a way of visualizing the vibrations of *m*DFB expressed in terms of those of benzene via a Duschinsky matrix approach. This method allows one set of vibrations to be fully expressed as linear combinations of another set of vibrations. The shading, noted in the figure caption, indicates the degree of similarity between the vibrations in the two molecules, with black meaning the vibrations are identical, and shades of grey quantitatively representing the degree of similarity. The data we extract from the Duschinsky matrix is also presented in a different form in Table 1.We have previously noted that there are some caveats regarding setting up the Duschinsky matrix, in terms of which axis system is chosen, and the reader is directed to Ref. [7] for these; here we shall move onto the results of our comparisons. The key conclusion from both Figure 1 and Table 1 is that in many cases the modes of one molecule can only be expressed as significant mixtures of those of the other. Hence, in the majority of cases, it is not possible to associate a single Wilson label with a particular mode of *m*DFB leading us to, once again, conclude that the Wilson labels are not suitable labels.

We then move on to compare the modes of *m*DFB with those of monofluorobenzene (FBz) (with the latter using the M_i labels of Ref. [5]) using the same approach. Figure 2 once again shows a Duschinsky matrix, allowing us to ascertain the degree of mixing between the vibrational modes. We have placed both molecules in the *yz* plane with the *z* axis passing

through the C-F bond in FBz and passing through the same C-H bond in *m*DFB as before, this is shown in Fig. 2. This separates the vibrations of both molecules into the a_1, a_2, b_1 and b_2 C_{2v} symmetry classes, and no mixing occurs between different classes. We present a breakdown of the *m*DFB vibrations in terms of those of the monosubstituted vibrations, employing the M_i labels, in Table 1. As can be seen from both Fig. 2 and Table 1, many of the *m*DFB vibrations are formed from significant mixtures of the FBz vibrations, with only a small number of vibrations remaining largely unchanged and therefore, unsurprisingly given the conclusions for this approach for both the *para*- and *ortho*-disubstituted benzene molecules, it is apparent that one cannot use the monosubstituted benzene vibrational labels to describe the vibrations in *m*DFB.

We now consider how the vibrations of benzene evolve into those of *m*DFB as we artificially change the mass of two hydrogen atoms in the *meta*- positions stepwise, from 1 amu through 19 amu. This mass correlation approach maintains a constant force field and hence neglects any electronic effects on the vibrational wavenumbers. We may, therefore, obtain a mass-only view of any changes to the benzene vibrations. We once again align the molecules (as we did above) so that the vibrations are separated into the C_{2v} symmetry classes. Figure 3 shows the plot for the in-plane a_1 and b_2 symmetry vibrations with the full range of wavenumbers shown, while Figure 4 shows all four of the C_{2v} symmetry classes, but with the omission of the high-wavenumber vibrations for the a_1 and b_2 classes. We first consider the evolution of the benzene vibrations to those of *m*DFB, which can be seen when moving from the centre of the diagram towards the left-hand side of each plot in Figs. 3 and 4. The same trends can be seen here as were previously seen in Refs. [6] and [7] in that there are stark changes in wavenumber as the mass changes, particularly within the first 10 amu. There are also a number of curves which appear to undergo “avoided crossings”. We note that when this occurs the vibrations involved are seen to become mixtures of one another, but that this mixing settles down when the curves separate again after the crossing. After about 10 amu, most of the curves start to level off, and we describe this as the point at which the normal modes stabilize and remain largely unchanged with any further mass change. In terms of the evolution of the vibrations of benzene to those of *para*-disubstituted benzenes, similar trends were seen [6], and the reader is directed to this work for a more in-depth analysis; similar comments apply to *ortho*-disubstituted benzenes [7]. This confirms that the *meta*-disubstituted benzenes are also not adequately represented by the Wilson labels.

We have previously discussed in Ref. [7] why we cannot use the ${}^{p}D_i$ labels for *ortho*-disubstituted benzenes and vice versa. The right hand side of Figures 3 and 4 each display the evolution of benzene to *p*DFB via the same stepwise change of mass of the indicated hydrogen atoms shown in the diagram. To allow for straightforward comparison, we have aligned the axis system in such a way that both molecules maintain the same C_{2v} symmetry elements as the mass is varied, allowing the direct correlation of the *p*DFB vibrations on the right-hand side with those of the *m*DFB vibrations on the left. This axis system is the same as the one employed in Ref. [6], but not the same as the one employed in Ref. [7]. The choice of this particular C_2 axis for *p*DFB leads to $3a_2 + 6b_1$ out-of-plane modes and $11a_1 + 10b_2$ in-plane modes and these match those of *m*DFB, allowing for a mode-by-mode comparison. *p*DFB itself belongs to the D_{2h} point group, and so each vibration has *u* or *g* symmetry – we have used colour within both Fig. 3 and Fig. 4 to allow the reader to identify which lines correspond to which symmetry class. Importantly, lines of the same colour, and thus the same symmetry, are not allowed to cross and will undergo avoided crossings (such as with ${}^{p}D_{28}$ and ${}^{p}D_{29}$ in Fig. 4); on the other hand, lines of different colours (e.g. ${}^{p}D_{18}$ and ${}^{p}D_{19}$) can cross. In each of the left-hand quadrants of each diagram in Fig. 4 no lines can cross as they are all of the same C_{2v} symmetry class.

The mass-correlation curves, as well as the mixings indicated in Table 1, may be used complementarily in order to gain insight into the mixings occurring between different vibrations. Perhaps the most important point is that, if one traces the curves in Figs. 3 and 4 from one side (*p*DFB) to the other side (*m*DFB), there are a number of avoided crossings occurring and, therefore, significant mixing of the modes. In Fig. 5 we show a Duschinsky matrix comparing the vibrational modes of *p*DFB to those of *m*DFB and it is noticeable that a number of the vibrations are heavily mixed and, therefore, there is not a 1:1 correspondence between the *p*DFB and *m*DFB vibrations. Thus we make an analogous conclusion to that in Ref. [7], that the vibrations of *m*DFB and *p*DFB also cannot be consistently labelled using a single scheme.

We also show that we cannot use the ${}^{o}D_i$ labels of Ref. [7] as a way of labelling the modes of *m*DFB. Again, the Duschinsky matrix approach requires that the each atom for *o*DFB be aligned with another atom of *m*DFB. With *m*DFB and *o*DFB, however, it is not possible to align so that the same C_{2v} axis system is maintained for both molecules, since this would require the *z* axis both to intersect the C-C bond bridging the C-F bonds in *o*DFB and pass through the C-H bond between the two C-F bonds in *m*DFB. The same C_{2v} symmetry elements can therefore not be achieved for both molecules and, as a result, mixing of a_1 with b_2 and a_2 with

b_1 modes is seen – see Ref. [7] for a discussion of these points when comparing the vibrations of *ortho*-disubstituted benzenes with those of the corresponding *para* species. We show comparisons for two axis systems in Figure 6 where, in each case, we have aligned one of the C-F bonds in each molecule. It may clearly be seen that there is not a 1:1 correspondence between the vibrations of the *ortho* and *meta* species.

In summary, we have previously shown that we require a separate labelling scheme for each of the *mono*-substituted, *para*-, and *ortho*-disubstituted benzenes; here, we have demonstrated the same for *meta*-disubstituted benzenes.

We now move on to describing the use of the vibrational modes of *m*DFB as a basis for labelling the *meta*-disubstituted benzenes. Similar to Refs [2], [6] and [7], we present mass correlation diagrams in Fig. 7. These employ the force field of *m*DFB while changing the masses of both F atoms simultaneously to match that of each of the halogens, where we choose the most abundant isotope in each case. The curves all appear to remain mostly flat, with some lines tending towards slightly lower wavenumber with mass. There are no signs of avoided crossings in the curves and, hence, no obvious signs of significant mixing and hence no significant changes in vibrational character. Similarly, in Fig. 8, we employ the force field of *m*DFB and vary the mass of a single F atom to match the other halogens. The same trend is noted in that, although there is a decrease in the wavenumber of some vibrations, the vibrational character does not significantly change. This is still ostensibly the case, even though the molecular point group symmetry has now lowered to C_s for these asymmetric substitutions, and there are now avoided crossings, such as between the vibrations labelled 19 and 20. This is also confirmed in both cases by the relevant Duschinsky matrices which show largely diagonal character which we do not show here. As a result of this, we use the normal modes of *m*DFB as a basis for labelling the vibrational modes of *meta*-disubstituted benzenes. As in the *ortho*-disubstituted benzenes [7], we desire the labels to be widely applicable to symmetric and asymmetric *meta*-disubstituted benzenes, and so we construct these labels in the C_s point group denoting them as ${}^{m}D_i$ in a similar way that we have done for the other two isomers, where the pre-superscript denotes '*meta*' and the post-subscript denotes the number of the vibration; the pre-superscript is generally only required when distinction between isomers is needed. We restrict our labels to the phenyl-ring localized modes, and so any substituents are treated as point masses and their localized modes are treated separately.

In summary, we propose the use of the ${}^{m}D_i$ labels for the phenyl-ring-localized vibrations of *meta*-disubstituted benzenes. We have included a diagrammatic representation of each vibrational mode in Fig. 9. It is straightforward to assign a label to a vibration by simply visualizing the motion via quantum chemical calculations, or through analysis of the mass correlation trends or via a Duschinsky matrix comparison. There are, however, two pairs of modes which require an element of caution. As we have seen previously in both *ortho*- and *para*-disubstituted benzene molecules, there are cases whereby modes that are symmetric and asymmetric stretches in symmetrically-substituted molecules, evolve into localized stretching modes. In Fig. 10, the D_{10} and D_{13}, and D_{18} and D_{19}, pairs of vibrations are shown, and can be seen to demonstrate localized character; this will occur when the difference in mass for the substituents is large. What is noticeable is that D_{10}, which is a symmetric in-phase substituent stretch, and D_{13}, which is an asymmetric, out-of-phase stretch, become localized C-X and C-Y stretches (where X and Y denote different substituents). Similarly, D_{18} has symmetric in-phase stretch character whereas D_{19} has out-of-phase asymmetric stretch character, and these modes become localized C-X and C-Y stretches. This will be discussed further in the below, in relation to particular substituents.

4. Assigning the vibrations

We now consider families of different *meta*-disubstituted benzenes and for each we present a summary of both calculated and experimental vibrational wavenumbers, as well as discussing previous assignments and any changes that we have made. We consider symmetrically disubstituted benzenes involving halogen atoms, OH and CH_3 groups; and asymmetric dihalobenzenes, halotoluenes, halophenols and cresol.

4.1 Symmetric disubstituted benzenes

A summary of both experimental and calculated vibrational wavenumbers can be found in Table 2. *m*DFB, in its ground electronic state ($\tilde{X}^1A_1$), has C_{2v} symmetry and 30 normal vibrational modes. Most experimental data for the dihalogens have been taken from a summary by Green [21], where the presented data have been extracted from previous liquid or solution phase infrared studies [22,23,24]; available Raman studies from Refs. [25,26,27] are also summarized in Ref. 20. In Table 2, for consistency, we favour the infrared values over the Raman values where both are available. We also present updated experimental values for *m*DFB, which we extract from the jet-cooled dispersed fluorescence study by Graham and Kable [28]; we use values taken from gas-phase studies where possible, as these are directly

comparable to our calculated values since they are not affected by perturbations due to solvent effects. Notably, in a few cases, we have re-ordered the vibrations to give like-motions the same ${}^{m}D_i$ label; the wavenumber ordering for some vibrations may therefore change from that of *m*DFB – the experimental values have also been switched to take into account these changes. To maintain our objective of the ${}^{m}D_i$ labels being applicable to all *meta*-disubstituted benzenes, we have separated the vibrations into *a′* and *a″* symmetry; but also, for clarity, in Table 2 we also give the C_{2v} Mulliken label that was used in Ref. 28. Experimental vibrational wavenumbers for *m*DClB, *m*DBrB, *m*DIB and *meta*-xylene (*m*Xyl) are all also extracted from the review by Green (Ref. 20). (Note that the abbreviations for the molecules follow the same logic as used above, with the halogen chemical symbol employed as appropriate.)

There have been several studies on resorcinol by Wilson [29], Kudchadker et al. [30] as well as Hidalgo and Otero [31]; we have preferred the gas phase values recorded by Wilson where available. There are, however, a number of uncertain and/or incomplete assignments and so we have also used a number of values from Ref. [30] when necessary. We have made our assignments of the vibrations taking account of the given symmetry from the papers, the comments noted by the authors, as well as through comparison with calculated data. The conformers employed in the calculations for resorcinol and *m*Xyl are given in the footnote of Table 2.

We present our calculated wavenumbers in Table 2 and, for the most part, there is very good agreement between theory and experiment, with only a small number of missing experimental values. In the majority of cases, the vibrational modes are fairly straightforward to identify across the family of substituted benzenes. Many of the experimental assignments deduced the symmetry of each vibrational mode via the band profile and/or comparing infrared and Raman activity. We note that the ordering of vibrations changes for the heavier dihalogens between D_{10} and D_{14}, as well as between D_{18} and D_{20} – this is apparent because of the same label being used for the same vibration, and arises from some energetically-close vibrations undergoing small changes in vibrational wavenumber with increasing substituent mass. We also note that the calculated and experimental [20] values for the D_{19} vibration of *m*DIB are not in good agreement, 308 cm^{-1} and 164 cm^{-1}, respectively, and we conclude that the experimental value is incorrect. It was noted in Ref. 20 that there were two weak bands observed at 1265 cm^{-1} and 1243 cm^{-1} either of which could be assigned to D_{11}, we have preferred 1243 cm^{-1} as it more closely matches our calculated value. Assignments for the dihalogens are otherwise consistent with the calculated data for the explicit molecules presented in Table 2, and we therefore make

no further changes. Fig. 7 also shows a mass correlation plot where we compare experimental values to the calculated ones obtained with the *m*DFB force-field and using artificial isotopes – in many cases the plots shows a high degree of concurrence between the experimental and calculated wavenumbers and suggests electronic effects are generally small. In cases where there is some deviation, this is thought to be indicative of electronic changes, such as variation in the force constant of one or more bonds; these still result in largely similar motions (but see the asymmetric cases below).

For *m*Xyl, infrared studies from the liquid phase and their corresponding assignments from various studies [32,33,34] have been summarized in Green [20]. Selco and Carrick [35] have also performed a jet-cooled emission study. We favour values from the emission study over the infrared, when available, for the same reasons mentioned above. The correspondence between calculated and experimental data are, once again, mostly good. In Refs. [20] and [35] a C-C bending mode is assigned a value of 1467 cm^{-1} and 1460 cm^{-1}, respectively; however, we do not calculate a value close to these with our closest calculated value being 1408 cm^{-1} (D_8). This poor agreement suggests that neither of these experimental values matches a calculated vibrational fundamental, and we therefore choose not to associate those experimental values with D_8.

4.2 Asymmetric dihalobenzenes

Table 3 presents a summary of the available experimental vibrational wavenumbers as well as our calculated values. The experimental data for the asymmetric *meta*-dihalobenzenes has been taken from Ref. [20] which is, once again, mostly data collected from liquid phase infrared spectroscopy studies. Any gaps in the IR study have been filled with Raman studies from Ref. [36]. As noted above, to allow for comparison between all families of *meta*-disubstituted benzenes, we have employed the same ${}^{m}D_{\mathrm{i}}$ labels despite the symmetry of these molecules being different to those of the symmetric *meta*-disubstituted benzenes. Where necessary, once again we have changed the ordering of the corresponding experimental vibrational wavenumbers. There only appear to be a small number of missing experimental values and we see that, in general, the agreement with the calculated values is mostly very good. As in the symmetric *meta*-disubstituted benzenes, we see that the wavenumber ordering of the vibrations changes between D_9 and D_{14} as well as D_{18} and D_{20} compared to *m*DFB. We note, however, that the vibrational modes themselves are mostly unchanged and can be fairly obviously assigned, apart from the cases where local modes form upon substitution, discussed below.

Interestingly, we find the agreement between the experimental and calculated values of 202 cm^{-1} and 155 cm^{-1} for D_{21} of *m*ClIB as well as between the corresponding values, 147 cm^{-1} and 106 cm^{-1}, for *m*BrIB is fairly poor, and hence conclude those assignments were incorrect. As we have previously noted in Refs. [6] and [7], we did not always see the symmetric and asymmetric C-X stretching modes of a symmetrically-substituted benzene evolve into localized C-X and C-Y stretches in the asymmetric cases, as the mass of one of the substituents increased. The localization, where seen, has been indicated in Table 3. As in previous cases, [6, 7] we have consistently applied the D_{10} label to the higher-wavenumber C-X stretch, and D_{13} to the lower-wavenumber C-Y stretch. We also note that D_{18} and D_{19} also exhibit a similar degree of localization, and we have labelled these similarly in Table 3. (The main difference between the D_{10} and D_{18} vibrations is the in- and out-of-phase stretch motions of the two C-H groups that are positioned vertically in Figure 10; with similar correspondences between D_{13} and D_{19}, albeit reversed.) The localization is not always complete, but the extent is related to the difference in masses, with the highest degree of localization being seen when X = F and Y = I. We note that when the localization is not clear, such as when X = Cl or Br, we have labelled the vibrations as asymmetric or symmetric stretches instead. We note from the mass correlation diagrams in Figure 8 that some deviation is seen between the lines calculated with a fixed force field and the experimental data points; this indicates that some force constants are indeed changing, although the motion remains very similar.

4.3 meta-halotoluenes

A summary of all available experimental values for the four *meta*-halotoluenes considered, and our present calculated vibrational wavenumbers, is shown in Table 4, where the lowest calculated energy conformer is indicated in the footnote of the table. The experimental values, once again, are a combination of liquid phase IR and Raman studies both summarized by Green in Ref. [20], where Green extracted the Raman data from Ref. [24]. As before, we have given vibrations with similar motions the same $^{m}D_i$ label, which leads to the ordering of the vibrations changing in some places compared to those of *m*DFB – the experimental vibrational wavenumbers have also been changed to match. There are only a few missing vibrational wavenumbers, notably in the range of >3000 cm^{-1}. The agreement is generally good between calculated and experimental data; there are some notable discrepancies particularly for D_5, D_8, D_{10} and D_{19} where the differences seem fairly large. This may be due, in part, to some coupling between methyl-localized modes and ring-localized modes that we have previously noted in Refs. [2], [6] and [7]. (We remind the reader that the $^{m}D_i$ labels only cover ring-localized

vibrations and the methyl-group vibrations are treated as separate.) The differences between calculated and experimental values for the modes noted above stay relatively constant across the range of the *meta*-halotoluenes and it still remains relatively easy to track each vibrational mode across the given series of molecules.

Once again, we notice a degree of localization, which was prevalent in the asymmetric dihalobenzenes. In *m*DFB, the two pairs of vibrations, D_{10} and D_{13}, as well as D_{18} and D_{19}, constitute a symmetric and asymmetric C-F stretch. In the halotoluenes, localization occurs in most cases, to yield a C-Me stretch and a C-X stretch (X = halogen, Me = CH_3). We note that this is not the case in *m*FT, but does occur from *m*ClT onwards. We have reflected this observation in Table 4 where we always assign D_{10} and D_{18} (when appropriate) to the carbon-methyl (C-Me) stretch and the D_{13} and D_{19} to the carbon-halogen stretches (C-X).

4.4 meta-halophenols and meta-cresol

A summary of the available experimental and present calculated vibrational wavenumbers for the phenyl-localized vibrations of the *meta*-halophenols and *meta*-cresol are presented in Table 5. The conformer employed has once again been noted in the footnote of the table. The experimental values have been taken from Green [37], where a combination of solution and liquid phase IR values are given. Raman values have also been incorporated from Refs. [24] and [35]. We have given vibrations with similar motions the same ${}^{m}D_i$ label, which may lead to the ordering of the vibrations changing relative to that for *m*DFB – the experimental values have been reordered to reflect these changes. Once again the agreement between the calculated and experimental data are very good and the trends in the vibrations may be followed across the series of molecules. We again note that the hydroxyl group vibrations, as well as the methyl group vibrations of *meta*-cresol, do not form part of the ${}^{m}D_i$ labelling scheme and should be treated separately.

We see localization of the C-OH and C-X stretches in the D_{10} and D_{13} vibrations, as well as in the D_{18} and D_{19} modes. We use the D_{10} and D_{18} labels for the C-OH stretches, with D_{13} and D_{19} being used for the C-X stretches. The exception is for *m*FPhOH where we retain the symmetric/asymmetric labels as the degree of localization is not complete. This is very similar to the case of the *meta*-halotoluenes discussed above.

5. Conclusions

In the present work, we have shown that it is possible to label the phenyl-localized vibrations of a range of *meta*-disubstituted benzenes consistently, where vibrations with the same or very similar atomic motion are associated with the same label. Throughout the study, we see that the ordering of the vibrations changes between species as a result of differing mass effects relating to the substituents. This would mean that the application of the usual Mulliken (Herzberg) labelling scheme, even for the same family of molecules, would give different labels to vibrational modes with the same atomic motions. We have shown how the motions of *meta*-disubstituted benzenes are related to other species (benzene, monosubstituted benzenes, *para*-disubstituted benzenes and *ortho*-disubstituted benzenes), and shown that the vibrations are often heavily mixed versions of one another. This leads us to conclude that the vibrational motions of the *meta*-disubstituted benzenes are significantly different to those of the other isomers, and this means that different labelling schemes are required for each. It is worth noting that some caution is required when applying the labels as the centres of mass shift somewhat for differing isomers or in the case of asymmetric substitution. Although the *z*-axis remains fixed to the centre of mass, the changes in its position lead to distortions of the motions of some of the atoms to compensate. This issue proves not to be overly problematic, and it was still possible to trace the modes as a function of mass with a fixed force-field and to identify which vibrational mode corresponded to which $^{m}D_i$ label. As noted for the *para*- and *ortho*-disubstituted benzenes, significant localization occurs in pairs of modes involving symmetric and asymmetric substituent stretches.

We anticipate that this labelling scheme for *meta*-disubstituted benzenes will be useful in unearthing trends in vibrational activity between molecules, as we have noticed when examining the vibrationally resolved electronic and photoelectron spectra of both monosubstituted and *para*-disubstituted benzenes (see references cited above).

Acknowledgements

We are grateful to the EPSRC for funding via grant EP/L021366/1. The EPSRC and the University of Nottingham are thanked for studentships to A.A., D.J.K and W.D.T. We are grateful to the High Performance Computer resource at the University of Nottingham for the provision of computer time.

Table 1. Labelling schemes for the S_0 vibrations of *m*DFB

Mode[a]	Mulliken C_{2v}[b]	*m*DFB - Varsányi[c]	Mixed (Bz)[c,d]	Mixed (FBz)[e]
			a′	
$^mD_1\,(a_1)$	1	20b	20a, 7a, (2, 13)	M_6, M_{11}, (M_{10})
$^mD_2\,(a_1)$	2	2	2, 20a, (13)	M_2, M_{30}, (M_3)
$^mD_3\,(b_2)$	21	7a	**20b,** 7b	$\boldsymbol{M_{21}}$,(M_{14})
$^mD_4\,(a_1)$	3	20a	7a, 13, (20a)	$\boldsymbol{M_3}$,M_2
$^mD_5\,(a_1)$	4	9a	**9a**	$\boldsymbol{M_4}$
$^mD_6\,(b_2)$	22	9b	**9b**	$\boldsymbol{M_{22}}$
$^mD_7\,(b_2)$	23	18b	**18b**	$\boldsymbol{M_{23}}$
$^mD_8\,(a_1)$	5	18a	**18a**, (8a, 19a)	$\boldsymbol{M_5}$,(M_8)
$^mD_9\,(b_2)$	24	14	**15**, (3)	$\boldsymbol{M_{25}}$,(M_{24})
$^mD_{10}\,(a_1)$	6	13	1, (12, 13, 2, 18a, 7a, 20a)	M_9,(M_{30},M_2,M_5)
$^mD_{11}\,(b_2)$	25	3	**3**, (8b, 19b, 15, 14)	M_{24},M_{27},(M_{29})
$^mD_{12}\,(b_2)$	26	8b	14, 8b, (19b)	$\boldsymbol{M_{26}}$,(M_{29},M_{14})
$^mD_{13}\,(b_2)$	27	19b	8b, (19b, 7b, 20b, 6b, 18b)	M_{29}, (M_{14},M_{26})
$^mD_{14}\,(a_1)$	7	19a	**19a**, 8a	M_8,M_7,(M_6,M_9)
$^mD_{15}\,(a_1)$	8	12	**12**, 1	M_6,M_{10},(M_8)
$^mD_{16}\,(b_2)$	28	7b	19b, (6b, 7b, 20b, 14, 8b)	M_{28}, (M_{14},M_{27},M_{24},M_{25},M_{23})
$^mD_{17}\,(a_1)$	9	1	6a, (1, 12, 13 ,2)	M_9,M_{11},(M_{30},M_{10},M_2)
$^mD_{18}\,(a_1)$	10	6a	**6a**, (13, 2, 1)	M_{10},M_{11},(M_{30},M_9,M_2)
$^mD_{19}\,(b_2)$	29	6b	**6b**, (20b, 7b)	$\boldsymbol{M_{28}}$,(M_{14},M_{27},M_{29})
$^mD_{20}\,(b_2)$	30	15	(14, 3, 8b, 19b, 6b)	M_{27},(M_{24},M_{28},M_{25})
$^mD_{21}\,(a_1)$	11	8a	8a, 19a (18a)	M_7,M_8, (M_5)
			a″	
$^mD_{22}\,(b_1)$	15	4	**17b**, 5	$\boldsymbol{M_1}$,(M_{15})
$^mD_{23}\,(a_2)$	12	17a	**17a**, 10a	$\boldsymbol{M_{20}}$,(M_{12})
$^mD_{24}\,(b_1)$	16	17b	17b, 5, (11, 10b, 4)	(M_{15},M_{18},M_{17},M_{19},M_{16})
$^mD_{25}\,(b_1)$	17	11	**10b**, (11)	M_{16},(M_{15},M_{17},M_{19},M_1)
$^mD_{26}\,(b_1)$	18	5	**4**, (11)	M_{17},M_{16},(M_{18},M_{19})
$^mD_{27}\,(a_2)$	13	16a	16a, 10a, (17a)	M_{13},M_{12}
$^mD_{28}\,(b_1)$	19	16b	**16b**, (11)	M_{19},M_{18},(M_{17},M_{16},M_{15})
$^mD_{29}\,(a_2)$	14	10a	16a, (10a, 17a)	M_{13}, (M_{12},M_{20})
$^mD_{30}\,(b_1)$	20	10b	**17b**, 5	M_{18}, (M_{17}, M_{15})

[a] This work – see text. Labels are based on Mulliken numbering via the C_s symmetry group, with the C_{2v} symmetry class given in parentheses.

[b] Mulliken numbering via the C_{2v} symmetry group

[c] We have previously highlighted (Ref. 5) that several Wilson modes have been misnumbered throughout various texts in the last number of years. The following switches are often required: 8a↔9a, 8b↔9b, 18a↔19a, 18b↔19b, 3↔14. These switches have been made where these have occurred throughout the present work.

[d] These express the S_0 *m*DFB ^mD_i vibrational modes in terms of those of the benzene Wilson modes using a generalized Duschinsky approach involving artificial isotopologues – see text and Ref. 5 for more details. Values outside parentheses have mixing coefficients > 0.2 and are termed major contributions, with bolded values being dominant contributions (mixing coefficients > 0.5). Those inside parentheses have mixing coefficients between 0.05 and 0.2 and are termed minor contributions. If there are multiple contributions of each type, these are given in the order of largest contribution first. Vibrations with a mixing coefficient < 0.05 are ignored.

[e] These express the S_0 *m*DFB ^mD_i vibrational modes in terms of those of fluorobenzene, numbered as M_i modes, using a generalized Duschinsky approach involving artificial isotopologues – see text and Ref. 5 for more details. Values outside parentheses have mixing coefficients > 0.2 and are termed major contributions, with bolded values being dominant contributions (mixing coefficients > 0.5). Those inside parentheses have mixing coefficients between 0.05 and 0.2 and are termed minor contributions. If there are multiple contributions of each type, these are given in the order of largest contribution first. Vibrations with a mixing coefficient < 0.05 are ignored.

Table 2. Vibrational wavenumber for *m*-$C_6H_4X_2$ (X = F, Cl, Br, I, CH_3 and OH)

Mode		*m*Xyl		Resorcinol		*m*DFB		*m*DClB		*m*DBrB		*m*DIB	
D_i	C_{2v}	Expt[a]	Calc[b]	Expt[c]	Calc[b]	Expt[a]	Calc[b]	Expt[a]	Calc[b]	Expt[a]	Calc[b]	Expt[a]	Calc[b]
a′													
$^mD_1$ (a_1)	1	3052	3085	3064	3109	3095[f]	3122	3071	3124	3078	3123	3070	3119
$^mD_2$ (a_1)	2	3050	3050	3053	3078	3086	3116	-	3115	3058	3115	3070	3112
$^mD_3$ (b_2)	21	3032	3068	3039	3086	3086	3112	3095	3111	3078	3111	3055	3108
$^mD_4$ (a_1)	3	-	3059	3036	3068	-	3090	-	3087	-	3085	3046	3081
$^mD_5$ (a_1)	4	1584[d]	1579	1607	1594	1611[e]	1597	1577	1563	1567	1556	1553	1547
$^mD_6$ (b_2)	22	1613	1597	1614	1606	1613[e]	1592	1577	1561	1567	1553	1553	1542
$^mD_7$ (b_2)	23	1492	1482	1502	1487	1490	1475	1462	1450	1460	1446	1449	1441
$^mD_8$ (a_1)	5	-[f]	1408	1486	1469	1435	1439	1412	1399	1412	1392	1402	1384
$^mD_9$ (b_2)	24	1307[d]	1310	1304[j]	1309	1337	1304	1289	1290	1292	1288	1292	1290
$^mD_{10}$ (a_1)	7	1252[i]	1233	1299	1285	1292[c]	1255	1124[i]	1096	1059[i]	1046	1047	1030[i]
$^mD_{11}$ (b_2)	25	1266[d,i]	1282	1332	1332	1260	1252	1258[i]	1251	1256[i]	1253	1243	1249[i]
$^mD_{12}$ (b_2)	26	1154[i]	1145	1140	1141	1157[e]	1145	1161[i]	1152	1161[i]	1156	1176	1160[i]
$^mD_{13}$ (b_2)	27	1167[i]	1162	1133	1135	1120	1102	1080[h]	1065	1078[h]	1064	1075	1065[h]
$^mD_{14}$ (a_1)	6	1096[d]	1089	1075	1065	1068[e]	1058	1073	1063	1096	1086	1075	1085
$^mD_{15}$ (a_1)	8	1000[d]	987	1000[k]	984	1012[e]	994	997	987	992	983	993	978
$^mD_{16}$(b_2)	28	905	893	-	947	956[e]	941	784	760	726	710	692	685
$^mD_{17}$ (a_1)	9	724[d]	716	745	735	739[e]	726	663	655	646	640	639	632
$^mD_{18}$ (a_1)	10	537	527	565[k]	529	522	514	398[i]	386	287[i j]	279	201	227
$^mD_{19}$ (b_2)	29	514[d]	508	542[k]	514	513[e]	502	429[g h]	417	357[i]	346	-[f]	308
$^mD_{20}$ (b_2)	30	383[d]	393	494[k]	465	477[e]	467	365	355	308[j]	302	238	265
$^mD_{21}$ (a_1)	11	273[d]	267	356[k]	322	329[e]	320	198	190	159	125	109	92
a″													
$^mD_{22}$ (b_1)	15	968	972	956	952	957[e]	963	964	970	968	971	966	971
$^mD_{23}$ (a_2)	12	905[j]	888	837	841	876[e]	871	892	892	894	894	899	897
$^mD_{24}$ (b_1)	16	874[d]	880	816	833	857[e]	856	867	874	868	877	872	881
$^mD_{25}$ (b_1)	17	769[d]	768	768	752	771[e]	767	773	773	769	770	768	766
$^mD_{26}$ (b_1)	18	690	694	680	677	680[e]	671	672	672	669	672	670	666
$^mD_{27}$ (a_2)	13	538[j]	517	-	611	603[e]	597	532	533	518	512	502[h]	491
$^mD_{28}$(b_1)	19	433	433	458[k]	452	454[e]	455	433	432	433	426	417	418
$^mD_{29}$ (a_2)	14	226[g]	216	243[k]	228	252[e]	239	212[g]	197	199[g]	180	186[h]	165
$^mD_{30}$ (b_1)	20	204	194	200[k]	217	227[e]	222	175	162	132	140	98	123

[a] Infrared spectroscopy of the liquid unless otherwise indicated [20].

[b] B3LYP/aug-cc-pVTZ values scaled by 0.97 – this work (see text). For consistency with the following tables, we have noted the symmetric and asymmetric stretch nature of D_{10} and D_{13} as well as the D_{18} and D_{19} explicitly. The conformer used for *m*Xyl has both methyl groups eclipsed with respect to the phenyl ring, and rotated 180□ with respect to each other ("*trans*"). For resorcinol, the OH groups are in the plane of the phenyl ring, in a pseudo hydrogen-bonded arrangement.

[c] Wilson jet cooled dispersed fluorescence.

[d] Experimental values from a jet-cooled dispersed fluorescence study [35].

[e] A number of experimental values were derived by us from assignments and band positions given in the jet-cooled dispersed fluorescence study [28].

[f j] Poor agreement of the experimental value [21] with the calculated values leads us to conclude the experimental assignment was incorrect.

[g] Raman studies of the liquid [21].

[h] Infrared values via the solid state [21].

[i] Wavenumber ordering switched from Ref. [21].

[j] Inferred values from Ref. [21].
[k] From a summary of values used in thermochemical study by Kudchadker et al. [30].

Table 3. Vibrational wavenumber for *m*-C_6H_4XY: asymmetric *meta*-diahalobenzenes

Mode	*m*ClFB		*m*BrFB		*m*FIB		*m*BrClB		*m*ClIB		mBrIB	
	Expt[a]	Calc[b]	Expt[a]	Calc[b]	Expt[a]	Calc[b]	Expt[a]	Calc[b]	Expt[a]	Calc[b]	Expt[a]	Calc[b]
a′												
D_1	-	3122	3096	3120	3085	3117	3090	3122	3080	3120	3075	3117
D_2	3095	3116	3073	3115	3064	3113	3064	3115	3065	3113	3060	3112
D_3	-	3112	-	3110	-	3109	3049[d]	3111	3056	3109	3051	3107
D_4	-	3089	-	3087	-	3085	-	3085	-	3084	-	3082
D_5	1598	1581	1595	1578	1584	1574	1575	1560	1565	1556	1566	1552
D_6	1595	1578	1575	1573	1567	1568	1575	1556	1551	1551	1559	1547
D_7	1475	1463	1477	1460	1468	1458	1462	1448	1456	1446	1454	1442
D_8	1439	1417	1431	1413	1421	1408	1411	1395	1403	1391	1405	1388
D_9	1296	1296	1292	1294	1293	1291	1288	1288	1291	1289	1290	1287
D_{10}	1224[e] (C-F)	1203 (C-F)	1220[e] (C-F)	1200[e] (C-F)	1214[e] (C-F)	1198[e] (C-F)	1063[e] (sym)	1053[e] (sym)	1058[e] (sym)	1046[e] (sym)	1059[e] (sym)	1037[e] (sym)
D_{11}	1263[e]	1254	1266[e]	1255	1264[e]	1255	1260[e]	1252	1255[e]	1252	1253[e]	1251[e]
D_{12}	1155[e]	1143	1157[e]	1144	1158[e]	1147	1165[e]	1154	1164[e]	1157	1165[e]	1158[e]
D_{13}	1059[e] (C-Cl)	1049 (C-Cl)	1057[e] (C-Br)	1043 (C-Br)	1051[e] (C-I)	1039 (C-I)	1082[e] (asym)	1067 (asym)	1078[e] (asym)	1070 (asym)	1078[e] (asym)	1064[e] (asym)
D_{14}	1080[e]	1072	1081[e]	1073	1079[e]	1074	1106[e]	1089	1096[e]	1088	1086[e]	1085[e]
D_{15}	1002	991	1001	989	1000	988	997	985	990	983	998	980
D_{16}	880	865	859[d]	846	846	834	753	734	742	724	711	695
D_{17}	683	673	666	656	649	646	650	645	648	640	643	634
D_{18}	519 (C-F)	510 (C-F)	519 (C-F)	510 (C-F)	518 (C-F)	510 (C-F)	304[f] (sym)	294 (sym)	256[f] (sym)	251 (sym)	250[f] (sym)	242 (sym)
D_{19}	409[f] (C-Cl)	394 (C-Cl)	307[f] (C-Br)	299 (C-Br)	255[f] (C-I)	252 (C-I)	422[f] (asym)	406 (asym)	424[f] (asym)	405 (asym)	339[f] (asym)	329 (asym)
D_{20}	444[d f]	433	436[f]	425	439[f]	419	352[f]	343	340[f]	332	297[f]	290
D_{21}	245[d]	238	203	196	177	169	-[g]	155	150	136	-[g]	106
a″												
D_{22}	965	967	966	966	968	966	968	971	968	971	970	971
D_{23}	890[c]	883	882	885	888	888	894	894	895	897	898	898
D_{24}	858	864	858	862	860	862	872	874	868	876	870	874
D_{26}	774	772	773	770	773	770	775	771	771	770	769	768
D_{25}	672	673	671	671	672	669	674	671	672	671	670	668
D_{27}	565	566	554	554	542	544	515[d]	522	510	512	499	501
D_{28}	443	443	440	439	430	435	430	428	420	425	420	420
D_{29}	245	233	241	231	235	231	202	191	200	187	200[c]	174
D_{30}	189	177	174	158	161	142	163	148	144	136	114	128

[a] Infrared spectroscopy of the liquid unless otherwise indicated [21].

[b] B3LYP/aug-cc-pVTZ values scaled by 0.97 – this work (see text). For consistency with the following tables, we have noted the symmetric and asymmetric stretch nature of D_{10} and D_{13} as well as the D_{18} and D_{19} explicitly.

[c] Inferred values from Ref. [21].

[d] Raman studies of liquid from Ref. [21].

[e] Some of the vibrations D_{10}–D_{14} do not appear in the same wavenumber order as in *m*DFB. Vibrations that have similar motions have been given the same D_i label, and the experimental wavenumbers have been re-ordered to match this.

[f] Some of the vibrations D_{18}–D_{20} do not appear in the same wavenumber order as in *m*DFB. Vibrations that have similar motions have been given the same D_i label, and the experimental wavenumbers have been re-ordered to match this.

[g] Poor agreement of the experimental value with the calculated values leads us to conclude the experimental assignment is incorrect.

Table 4. Vibrational wavenumber for *m*-$C_6H_4XCH_3$: *meta*-halotoluenes

Mode	*m*FT		*m*ClT		*m*BrT		*m*IT	
	Expt[a]	Calc[b]	Expt[a]	Calc[b]	Expt[a]	Calc[b]	Expt[a]	Calc[b]
a′								
D_1	3081	3108	3085	3109	3109	3109	3080	3108
D_2	3060	3089	3064	3091	3090	3090	3058	3088
D_3		3087		3086	3085	3085		3084
D_4		3072		3070	3069	3069		3068
D_5	1595	1578	1578	1562	1557	1557	1564	1552
D_6	1623	1602	1604	1587	1585	1585	1593	1581
D_7	1492	1479	1478	1468	1466	1466	1466	1464
D_8	1460	1419	1467	1403	1402	1402	1416	1397
D_9	1295	1302	1296	1299	1298	1298	1300	1300
D_{10}	1251[c] (sym)	1240 (sym)	1221[c] (C-Me)	1194 (C-Me)	1192[c] (C-Me)	1192 (C-Me)	1211[c] (C-Me)	1191 (C-Me)
D_{11}	1266[c]	1271	1272[c]	1267	1268[c]	1268	1262[c]	1266
D_{12}	1160	1148	1164	1155	1157	1157	1168	1159
D_{13}	1143 (asym)	1127 (asym)	1096 (C-Cl)	1086 (C-Cl)	1060[c] (C-Br)	1060 (C-Br)	1063[c] (C-I)	1054 (C-I)
D_{14}	1079	1071	1079	1068	1089[c]	1089	1093[c]	1091
D_{15}	1003	989	1002	990	988	988	992	986
D_{16}	924	913	858	837	819	819	819	809
D_{17}	728	719	684	673	659	659	657	651
D_{18}	527 (sym)	519 (sym)	522 (C-Me)	511 (C-Me)	508 (C-Me)	508 (C-Me)	521 (C-Me)	502 (C-Me)
D_{19}	513 (asym)	505 (asym)	416 (C-Cl)	402 (C-Cl)	299[d] (C-Br)	299 (C-Br)	255[d] (C-I)	252 (C-I)
D_{20}	450[e]	435	387	376	372[d]	372	371[d]	362
D_{21}	296	285	221	226	190	190	173	166
a″								
D_{22}	970	968	976	972	969	972	970	973
D_{23}	886	886	898	895	896	896	896	897
D_{24}	858	860	869	870	868	872	873	875
D_{25}	778	774	776	772	770	769	768	767
D_{26}	683	683	684	683	680	682	681	681
D_{27}	556	557	522[f]	526	513	519	515	515
D_{28}	442	443	431	433	429	430	424	426
D_{29}	243	235	234	208	220	207	218	205
D_{30}	212	198	185	173	171	157	157	141

[a] Infrared spectroscopy of the liquid unless otherwise indicated [21].

[b] B3LYP/aug-cc-pVTZ values scaled by 0.97 – this work (see text). For consistency with the following tables, we have noted the symmetric and asymmetric stretch nature of D_{10} and D_{13} as well as the D_{18} and D_{19} explicitly. The conformer employed for *m*FT was eclipsed, while for the other three species it was staggered.

[c] Note that some of the vibrations D_{10}–D_{14} are not in the same wavenumber order as in *m*DFB. Vibrations with similar motions have been assigned the same D_i label. The corresponding experimental wavenumbers have been reordered to match the calculated ordering.

[d] Note that some of the vibrations D_{18}–D_{19} are not in the same wavenumber order as in *m*DFB. Vibrations with similar motions have been assigned the same D_i label. The corresponding experimental wavenumbers have been reordered to match the calculated ordering.
[e] Raman values of the liquid from Ref. [21].
[f] Inferred value from Ref. [21].

Table 5. Vibrational wavenumber for *m*-C_6H_4XOH: *meta*-halophenols and *meta*-cresol

Mode	*m*-cresol		*m*FPhOH		*m*ClPhOH		*m*BrPhOH		*m*IPhOH	
	Expt[a]	Calc[b]	Expt[a]	Calc[b]	Expt[a]	Calc[b]	Expt[a]	Calc[b]	Expt[a]	Calc[b]
					a′					
D_1	3080	3088	3074	3116	3057	3115	3054	3115	3052	3113
D_2	3042	3082	3049	3115	3073	3116	3072	3116	3073	3114
D_3	-	3071	-	3090	-	3088	-	3087	-	3086
D_4	-	3058	-	3067	-	3065	-	3065	-	3065
D_5	1600	1579	1603[e]	1593	1599[e]	1577	1584[e]	1574	1578[e]	1569
D_6	1614	1606	1619[e]	1602	1608[e]	1588	1599[e]	1583	1595[e]	1579
D_7	1490	1480	1491	1475	1489	1464	1484	1461	1480	1459
D_8	1462	1470	1461	1466	1462	1447	1455	1443	1438	1439
D_9	1281[e]	1299	1307	1312	1310	1303	1311	1299	1310	1298
D_{10}	1268[e] (C-OH)	1261 (C-OH)	1282[e] (sym)	1267 (sym)	1258[e] (C-OH)	1238 (C-OH)	1246[e] (C-OH)	1235 (C-OH)	1246[e] (C-OH)	1235 (C-OH)
D_{11}	1306[e]	1307	1295[e]	1286	1290[e]	1286	1294[e]	1286	1293[e]	1286
D_{12}	1163	1149	1154	1144	1154	1148	1154	1156	1157	1148
D_{13}	1149 (C-Me)	1138 (C-Me)	1134 (asym)	1112 (asym)	1069[e] (C-Cl)	1057 (C-Cl)	1062[e] (C-Br)	1050 (C-Br)	1056[e] (C-I)	1046 (C-I)
D_{14}	1085	1080	1072	1064	1088[e]	1076	1083[e]	1077	1082[e]	1079
D_{15}	1000	986	1004	989	998	984	996	983	994	981
D_{16}	930	918	954	943	888	870	864	851	851	840
D_{17}	733	722	738	729	687	676	667	659	653	651
D_{18}	536 (C-OH)	530 (C-OH)	530 (sym)	523 (sym)	526 (C-OH)	521 (C-OH)	531 (C-OH)	521 (C-OH)	529 (C-OH)	521 (C-OH)
D_{19}	518 (C-Me)	508 (C-Me)	515 (asym)	506 (asym)	410[f] (C-Cl)	395 (C-Cl)	308[f] (C-Br)	298 (C-Br)	255[c f] (C-I)	252 (C-I)
D_{20}	443	434	474	464	442[c, f]	431	439[f]	423	433[f]	435
D_{21}	297	288	327	321	249	240	206	197	178	172
					a″					
D_{22}	962	959	978	954	962	956	963	957	961	957
D_{23}	880	850	890[c]	847	885	859	878	859	867	860
D_{24}	855	874	849	858	859	865	864[c]	866	859[c]	870
D_{25}	776	765	766	757	771	761	771	760	771	761
D_{26}	685	686	676	675	676	675	676	674	675	674
D_{27}	560	564	590[c]	606	526[c]	574	531[c]	563	529[c]	552
D_{28}	443	443	454	455	442	442	435	439	429	435
D_{29}	246	225	241	234	233	225	231	224	231	223
D_{30}	211	199	226	218	189	178	170	159	157	143

[a] Infrared spectroscopy of the solution unless otherwise indicated [37].

[b] B3LYP/aug-cc-pVTZ values scaled by 0.97 – this work (see text). For consistency with the following tables, we have noted the symmetric and asymmetric stretch nature of D_{10} and D_{13} as well as the D_{18} and D_{19} explicitly. For *m*-fluorophenol the conformer was *trans*, with the OH pointing away from the halogen. For *m*-chloro-, *m*-bromo- and *m*-iodophenol the conformer was *cis*, with the OH pointing towards the halogen. For *m*-cresol, the OH points away from the methyl group, and the latter is staggered with respect to the phenyl ring, with the in-plane C-H pointing away from the O atom.

[c] Inferred values from Ref. [37].

[d] Note the vibrations D_5–D_6 are not in the same wavenumber order as in *m*DFB. Vibrations with similar motions have been assigned the same D_i label. The corresponding experimental wavenumbers have been reordered to match the calculated ordering.

[e] Note that some of the vibrations D_9–D_{14} are not in the same wavenumber order as in *m*DFB. Vibrations with similar motions have been assigned the same D_i label. The corresponding experimental wavenumbers have been reordered to match the calculated ordering.

[f] Note that some of the vibrations D_{18}–D_{20} are not in the same wavenumber order as in *m*DFB. Vibrations with similar motions have been assigned the same D_i label. The corresponding experimental wavenumbers have been reordered to match the calculated ordering.

Figure Captions

Figure 1: Generalized Duschinsky matrix showing how the vibrational modes of *m*DFB can be expressed in terms of the benzene ones – clearly significant mixing of the benzene modes occurs – see text for further discussion. Black shading indicates a normalized coefficient value of 1.00, while white indicates a value of 0.00, with grey shading indicating intermediate values, see text for details.

Figure 2: Generalized Duschinsky matrix showing how the vibrational modes of *m*DFB can be expressed in terms of the FBz ones – clearly significant mixing of the fluorobenzene modes occurs – see text for further discussion. Black shading indicates a normalized coefficient value of 1.00, while white indicates a value of 0.00, with grey shading indicating intermediate values, see text for details.

Figure 3: Mass-correlated vibrational wavenumbers showing how the vibrations of benzene (centre) evolve into those of *p*DFB (right) and *m*DFB (left) for the a_1 and b_2 vibrations, according to the indicated axis system. The force field of benzene is employed and the masses of the indicated hydrogen atoms are artificially varied from 1 to 19 amu in each case: ^{19}H in the figure indicates that the mass of the indicated hydrogen atom has been artificially changed to 19 amu. The *m*DFB labels have been included on the left, while on the right hand side the numbers refer to the $^{p}D_i$ modes as in Ref. [6]. An expanded region of both of these plots is shown as part of Figure 4, which also gives the Wilson modes in the centre. Note that we have used the same colour scheme and line type as employed in Figure 4.

Figure 4: Mass-correlated vibrational wavenumbers showing how the vibrations of benzene (centre) evolve into those of *p*DFB (right) and *m*DFB (left) for the vibrations separated into the four C_{2v} symmetry classes, according to the indicated axis system. The force field of benzene is employed and the masses of the indicated hydrogen atoms are artificially varied from 1 to 19 amu in each case: ^{19}H in the figure indicates that the mass of the indicated hydrogen atom has been artificially changed to 19 amu. The *m*DFB labels have been included on the left, on the right hand side the numbers refer to the $^{p}D_i$ modes from Ref. [6], while the Wilson modes are given in the centre. To aid the reader further, we have also indicated the appropriately colour-coded D_{2h} symmetry classes on the right-hand side of each panel. To allow comparison with Ref. [6], the purple/red lines indicate a_1 or a_2 symmetry vibrations, and blue/green lines indicate b_1 or b_2 vibrations, respectively – in each case now referring to the axis system used in that work. Further, vibrations on the right-hand side belong to the D_{2h} point group and so have *g*/*u* symmetry. See text for further discussion.

Figure 5: Generalized Duschinsky matrix showing how the vibrational modes of *m*DFB can be expressed in terms of the *p*DFB ones, with the molecules aligned as indicated – clearly significant mixing of the modes occurs – see text for further discussion. Black shading indicates a normalized coefficient value of 1.00, while white indicates a value of 0.00, with grey shading indicating intermediate values, see text for details. The alignment given allows separation of the modes for both

molecules into C_{2v} symmetry blocks, but we have also indicated the C_s symmetry partition that is appropriate for asymmetrically-substituted *ortho*-disubstituted benzenes, and as used for the construction of the ${}^{o}D_i$ labels.

Figure 6: Generalized Duschinsky matrix showing how the vibrational modes of *m*DFB can be expressed in terms of the *o*DFB ones, with the molecules aligned in two different ways as indicated – clearly significant mixing of the modes occurs in both cases – see text for further discussion. Black shading indicates a normalized coefficient value of 1.00, while white indicates a value of 0.00, with grey shading indicating intermediate values, see text for details.

Figure 7: Mass-correlated vibrational wavenumbers showing how the vibrations of *m*DFB (left-hand side) evolve as a function of mass in symmetric dihalo species; the highest wavenumber vibrations have been omitted (refer to Table 2). The vibrations have been separated into the two C_s symmetry classes, and in each class we have indicated *a* or *b* character with colour, as indicated. The force field of *m*DFB is employed and the masses of both fluorine atoms are artificially varied from 19 to 127 amu simultaneously in each case, to match the mass of the most abundant, naturally-occurring isotope of the halogens. The numbering of the ${}^{m}D_i$ labels is included on the left. Note that crossings between vibrations of different symmetry is allowed. The data points are the experimental values from Table 2, while the lines are the calculated values using a fixed force field for *m*DFB and using artificial isotopes.

Figure 8: Mass-correlated vibrational wavenumbers showing how the vibrations of *m*DFB (left-hand side) evolve as a function of mass in asymmetric dihalo species; the highest wavenumber vibrations have been omitted (refer to Table 3). The vibrations have been separated into the two C_s symmetry classes. The force field of *m*DFB is employed and the mass of the *ortho* fluorine atom is artificially varied from 19 to 127 amu in each case, to match the mass of the most abundant, naturally-occurring isotope of the halogens. The numbering of the ${}^{m}D_i$ labels is included on the left. (Note that the theoretical lines do not cross for D_{10} and D_{11}, as required; however, the experimental data indicate that there is a switch in the ordering of these two vibrations between *m*DFB and the cases where one fluorine atom is replaced by a heavier halogen – this effect is very small, and must be a result of subtle changes in the force field. The actual assignments of the vibrations, however, are based on the atomic motion.) The data points are the experimental values from Table 3, while the lines are the calculated values using a fixed force field for *m*DFB and using artificial isotopes.

Figure 9: Calculated vibrational modes for *m*DFB (B3LYP/aug-cc-pVTZ), labelled using the ${}^{m}D_i$ notation in the present work. See text for details.

Figure 10: A selection of calculated vibrational modes for *m*DFB and *m*FIB (B3LYP/aug-cc-pVTZ), labelled using the ${}^{m}D_i$ notation in the present work. (Green circles represent F and magenta circles represent I; C and H are both open circles.) Note that the D_{10} and D_{13} modes are largely the in-phase and out-of-phase C-F stretches for *m*DFB, while in *m*FIB these modes have evolved in being largely-localized C-F and C-I stretches, respectively; similar comments apply to D_{18} and D_{19}. See text for details and discussion.

Figure 1:

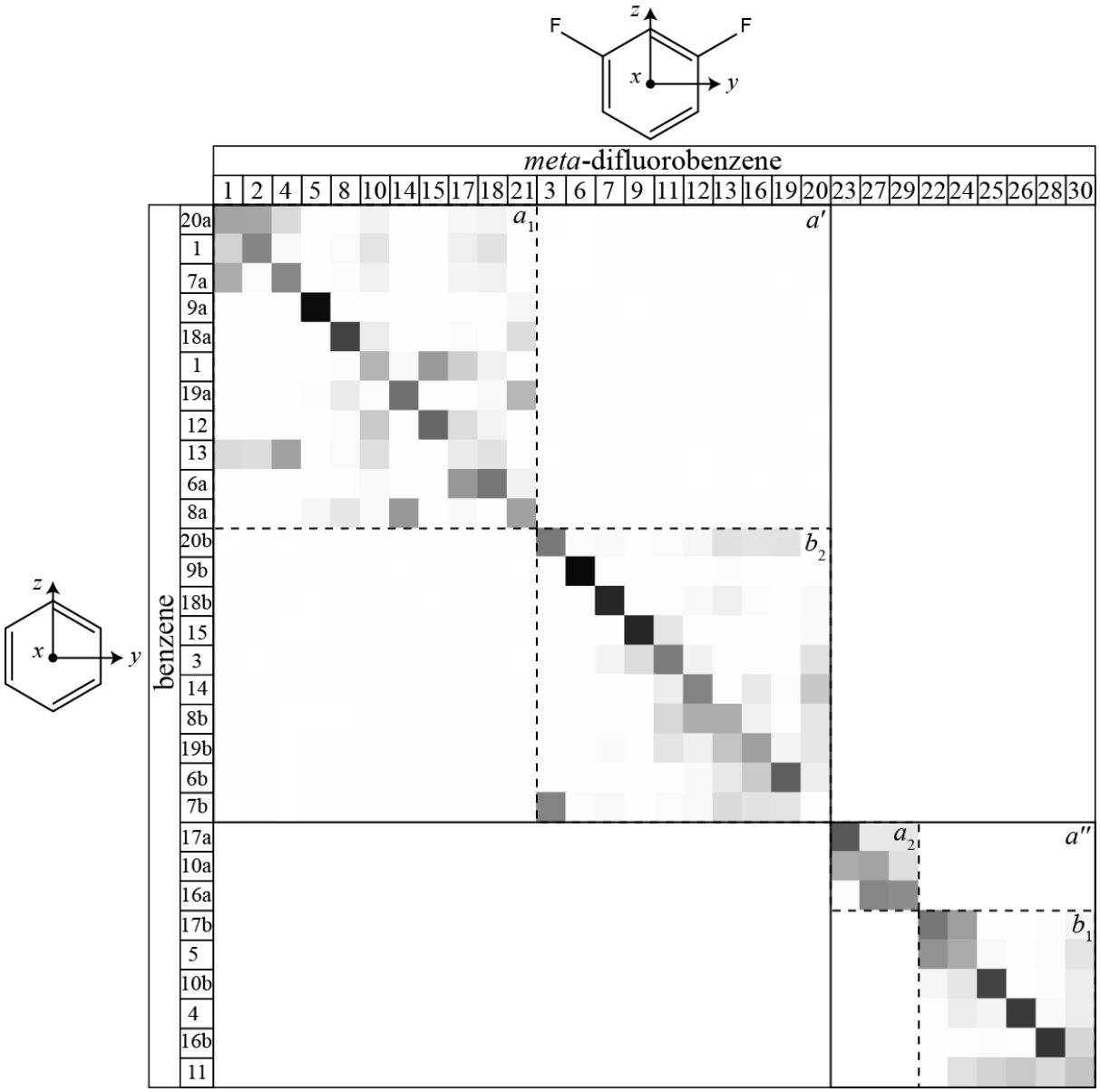
z
F
F
x
y
meta-difluorobenzene
1 2 4 5 8 10 14 15 17 18 21 3 6 7 9 11 12 13 16 19 20 23 27 29 22 24 25 26 28 30
benzene
20a 1 7a 9a 18a 1 19a 12 13 6a 8a
20b 9b 18b 15 3 14 8b 19b 6b 7b
17a 10a 16a 17b 5 10b 4 16b 11
a_1
a'
b_2
a_2
a''
b_1
z
x
y

Figure 2:

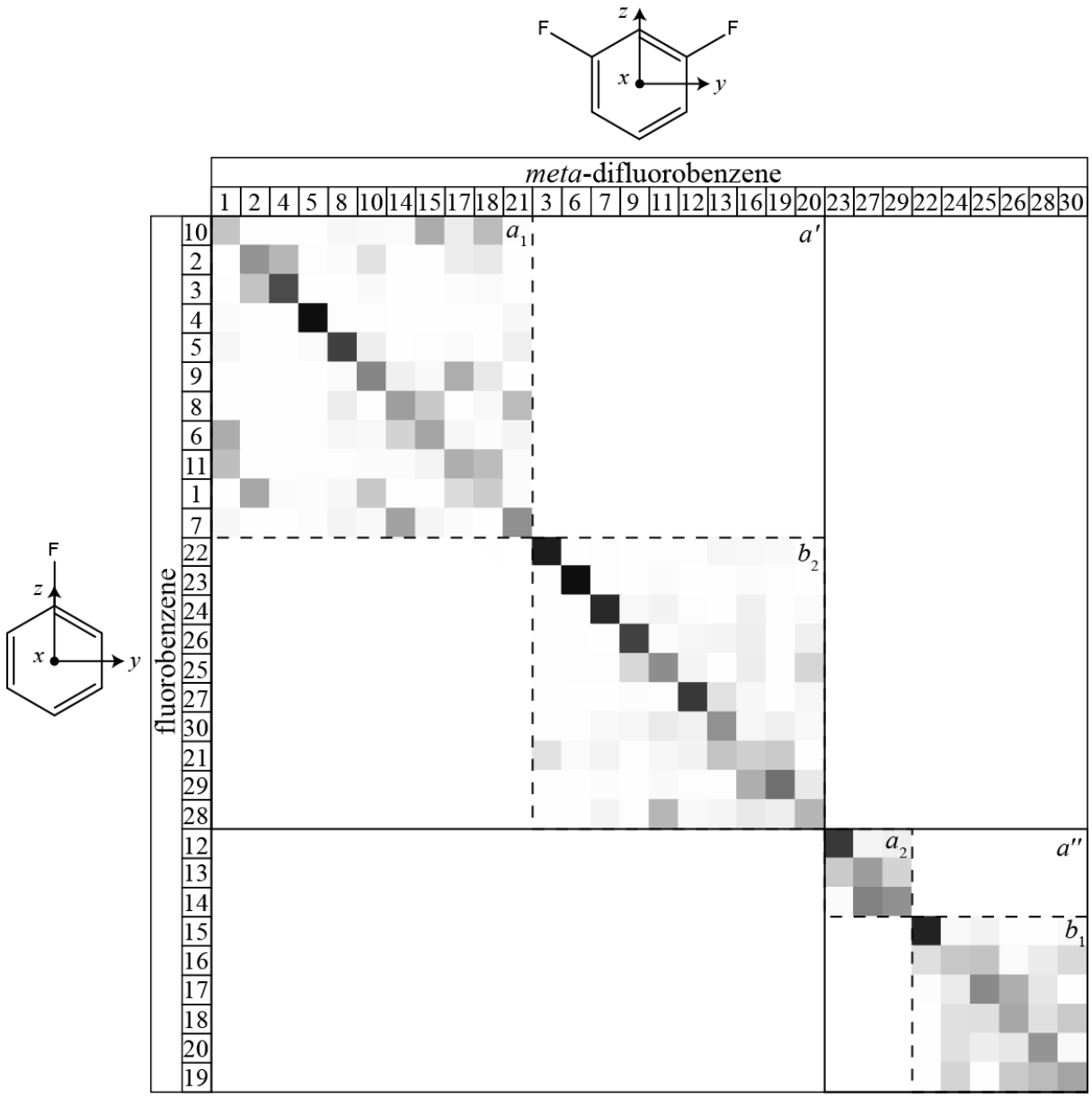
F
F
z
x
y
meta-difluorobenzene
1 2 4 5 8 10 14 15 17 18 21 3 6 7 9 11 12 13 16 19 20 23 27 29 22 24 25 26 28 30
fluorobenzene
10 2 3 4 5 9 8 6 11 1 7 22 23 24 26 25 27 30 21 29 28 12 13 14 15 16 17 18 20 19
a1
a′
b2
a2
a″
b1
F
z
x
y

Figure 3

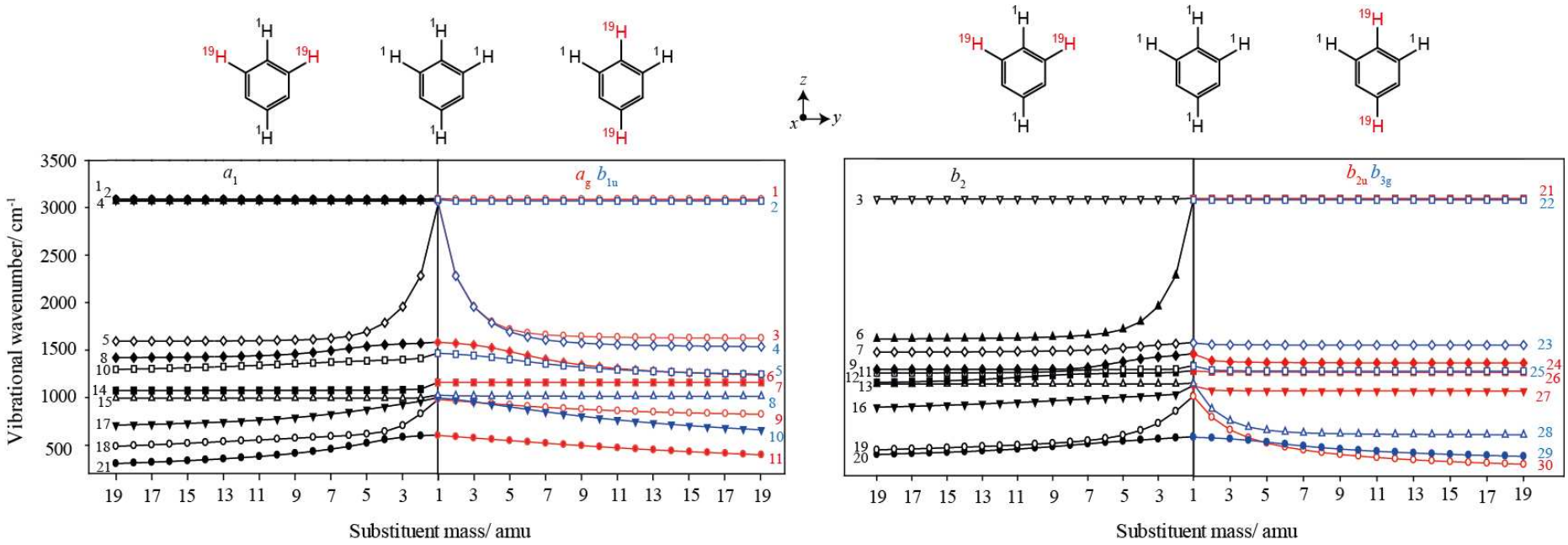
Vibrational wavenumber/ cm⁻¹
Substituent mass/ amu
Substituent mass/ amu
a1
ag b1u
b2
b2u b3g
z
x
y

Figure 4

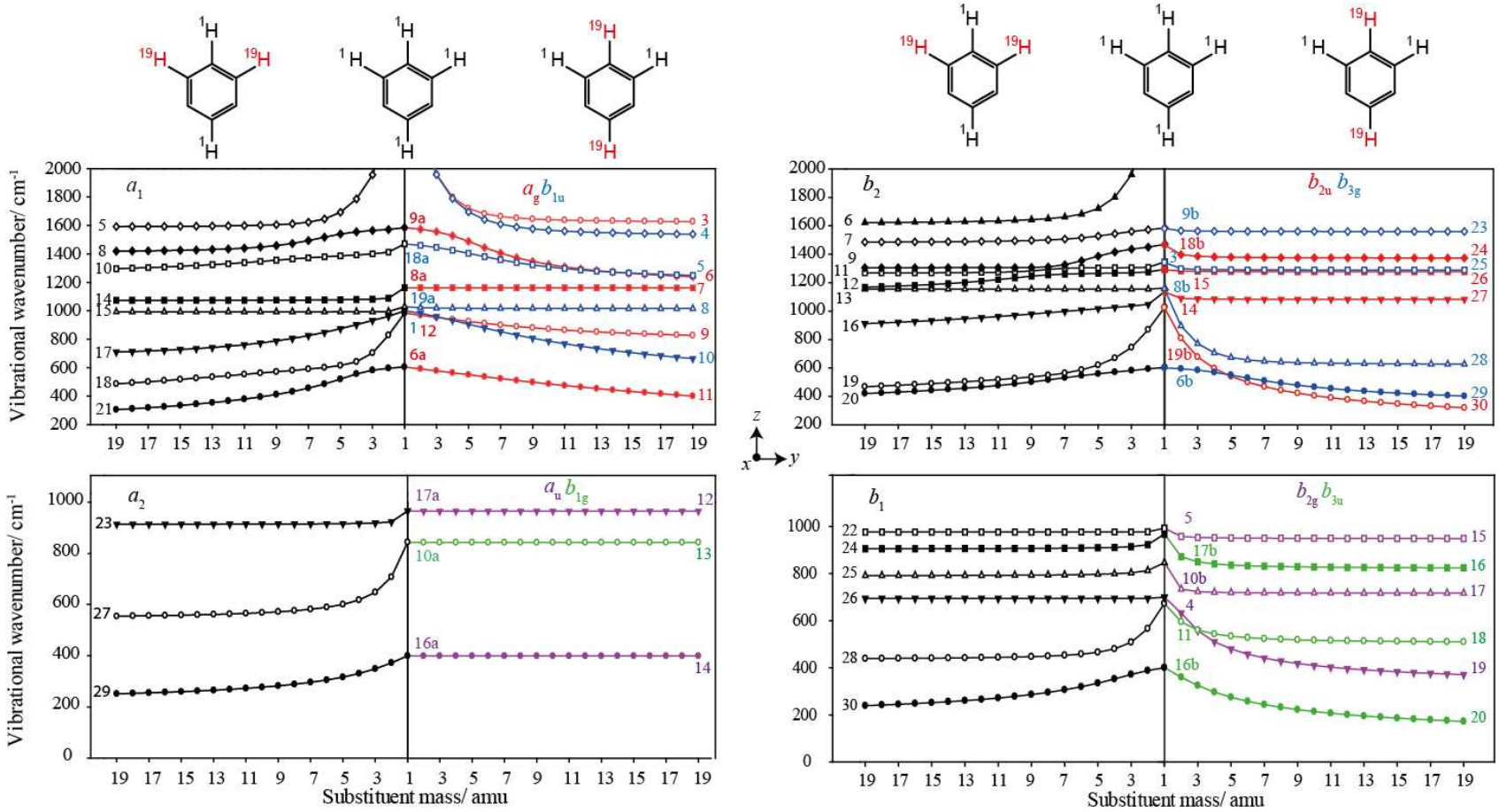
Vibrational wavenumber/ cm⁻¹
Substituent mass/ amu
a1
ag b1u
b2
b2u b3g
a2
au b1g
b1
b2g b3u
z
x
y

Figure 5

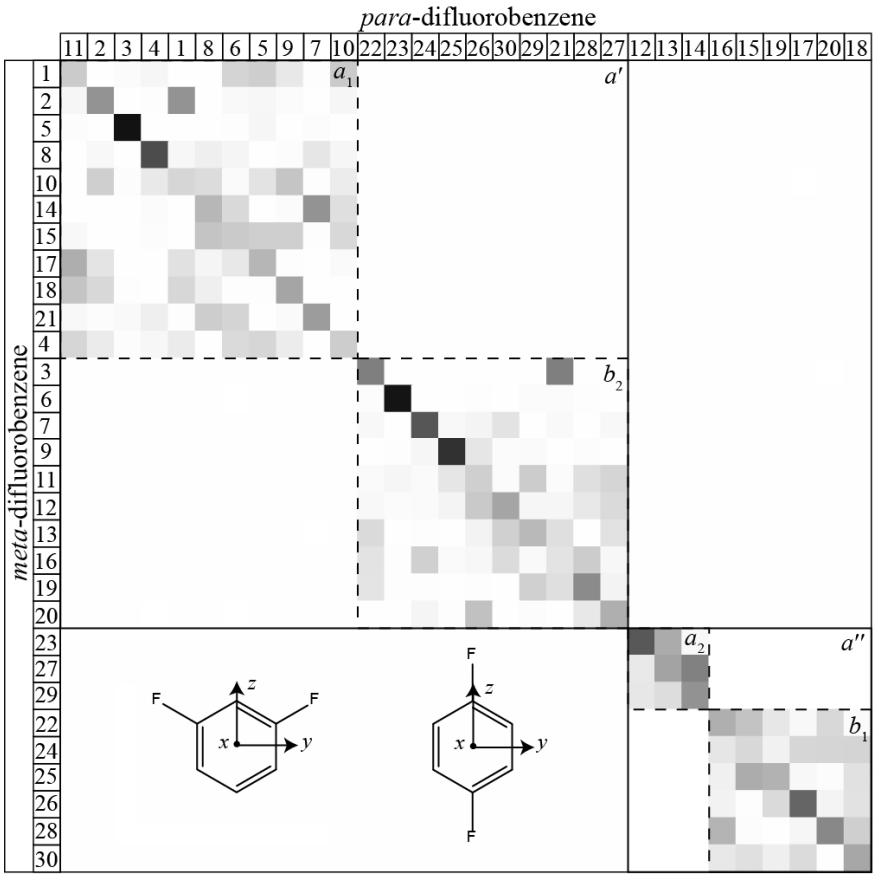
para-difluorobenzene
11 2 3 4 1 8 6 5 9 7 10 22 23 24 25 26 30 29 21 28 27 12 13 14 16 15 19 17 20 18
meta-difluorobenzene
1 2 5 8 10 14 15 17 18 21 4 3 6 7 9 11 12 13 16 19 20 23 27 29 22 24 25 26 28 30
a1
a′
b2
a2
a″
b1
F
F
z
x
y
F
z
x
y
F

Figure 6

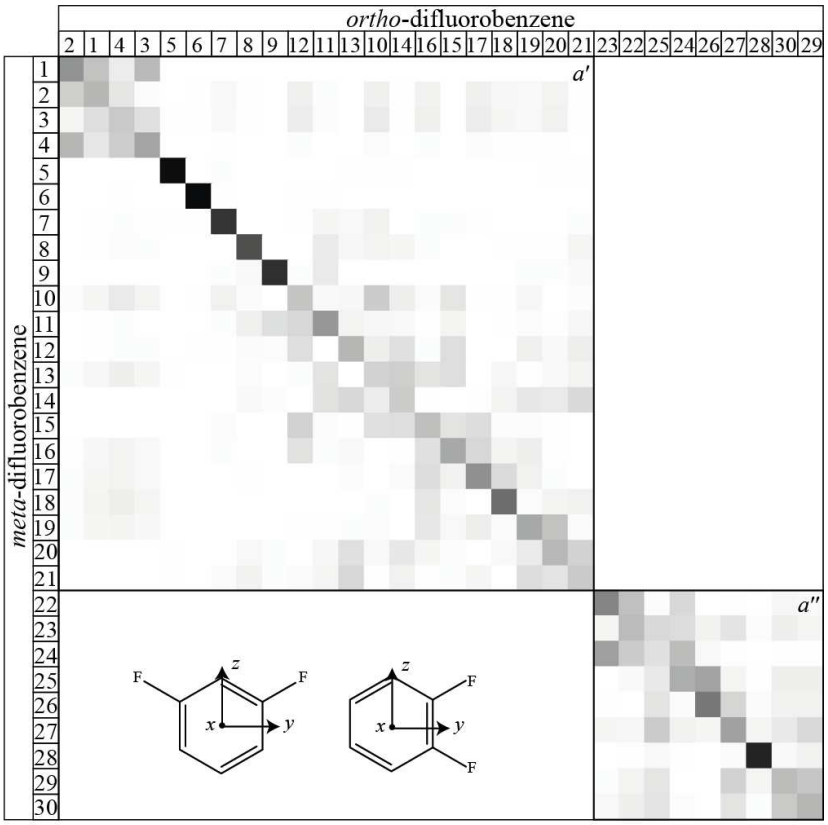
ortho-difluorobenzene
2 1 4 3 5 6 7 8 9 12 11 13 10 14 16 15 17 18 19 20 21 23 22 25 24 26 27 28 30 29
meta-difluorobenzene
1 2 3 4 5 6 7 8 9 10 11 12 13 14 15 16 17 18 19 20 21 22 23 24 25 26 27 28 29 30
a′
a″
F
F
z
x
y
F
F
z
x
y

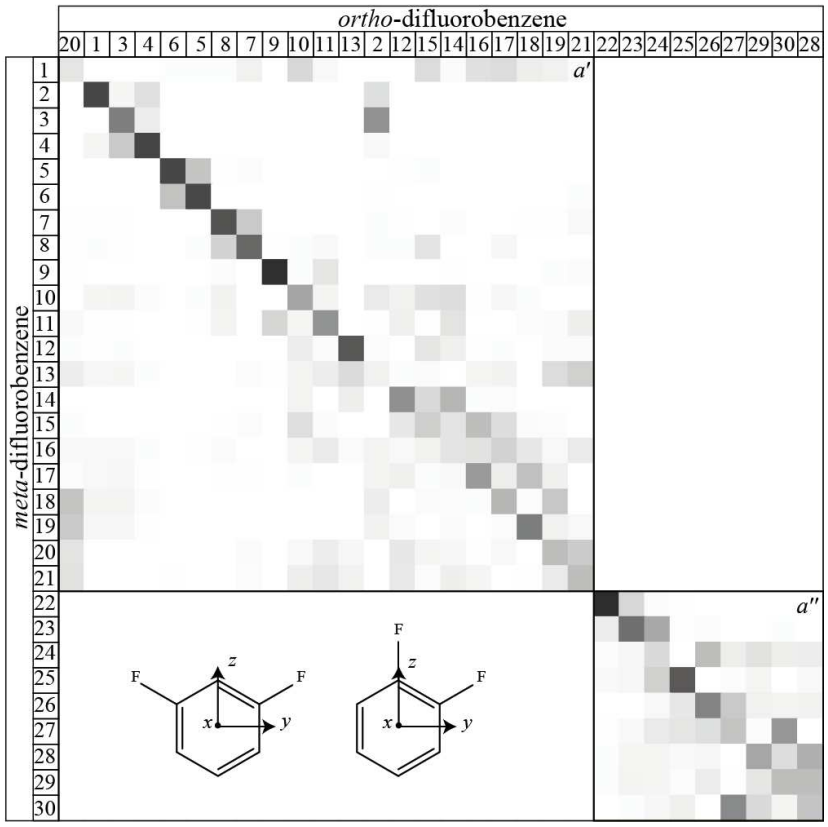
ortho-difluorobenzene
20 1 3 4 6 5 8 7 9 10 11 13 2 12 15 14 16 17 18 19 21 22 23 24 25 26 27 29 30 28
meta-difluorobenzene
1 2 3 4 5 6 7 8 9 10 11 12 13 14 15 16 17 18 19 20 21 22 23 24 25 26 27 28 29 30
a′
a″
F
F
z
x
y
F
F
z
x
y

Figure 7

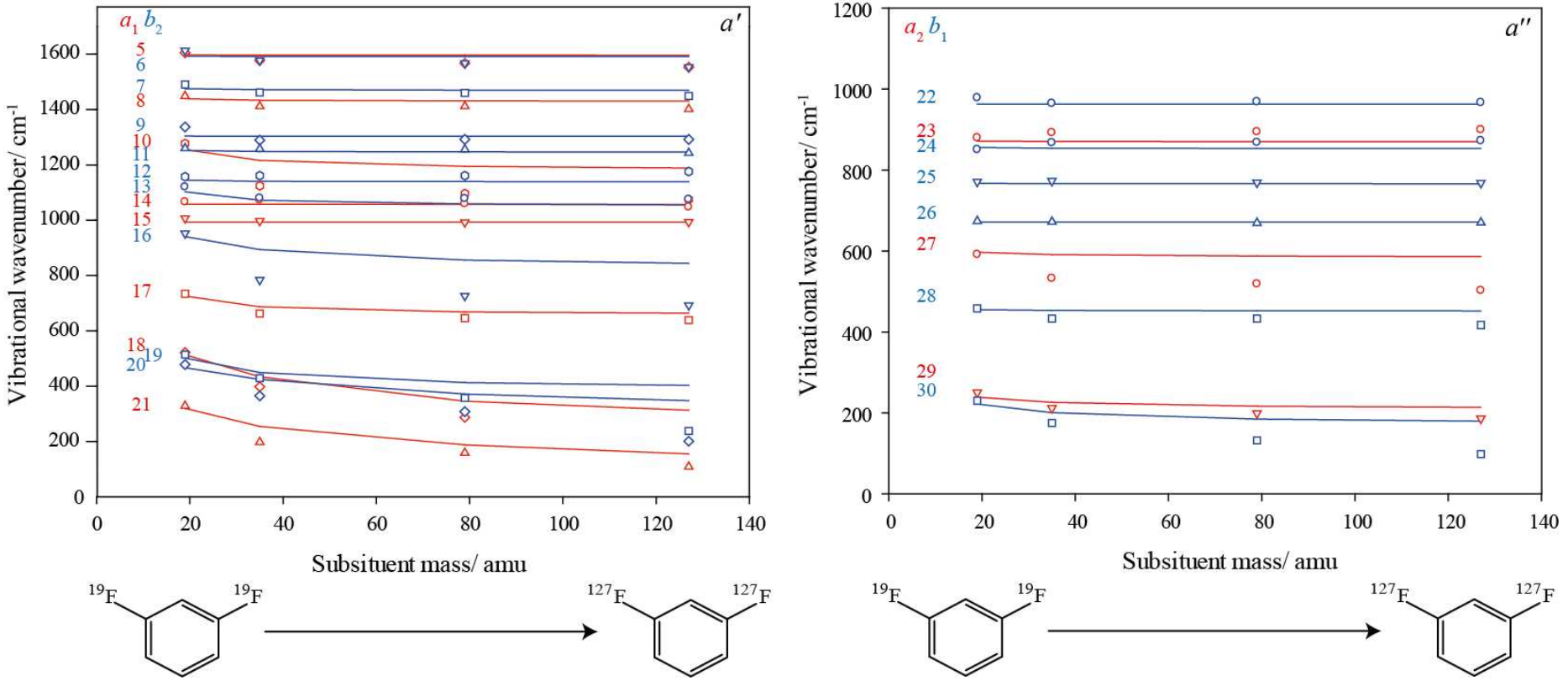
a' a1 b2
a'' a2 b1
Vibrational wavenumber/ cm-1
Subsituent mass/ amu
19F 19F
127F 127F

Figure 8

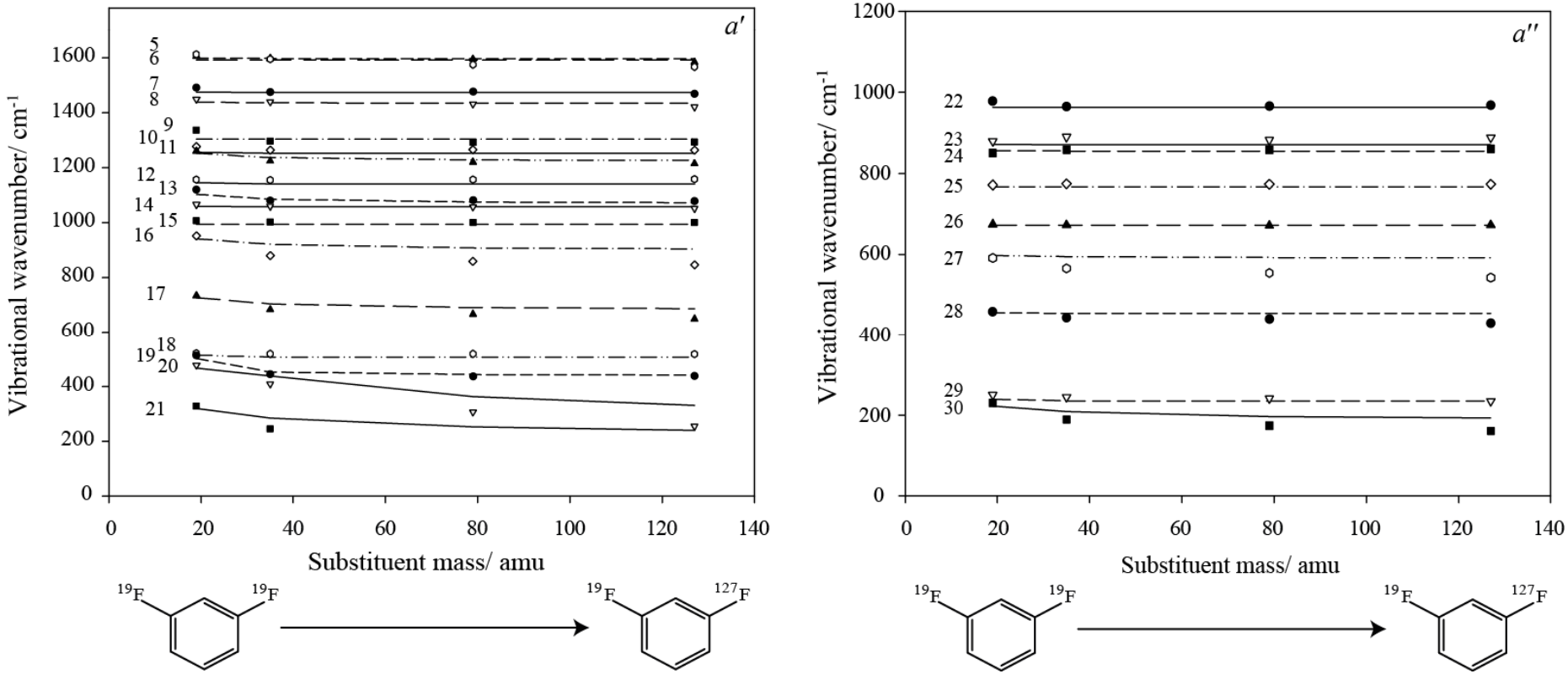
a′
Vibrational wavenumber/ cm-1
Substituent mass/ amu
5
6
7
8
9
10
11
12
13
14
15
16
17
18
19
20
21
19F
19F
19F
127F
a″
Vibrational wavenumber/ cm-1
Substituent mass/ amu
22
23
24
25
26
27
28
29
30
19F
19F
19F
127F

Figure 9

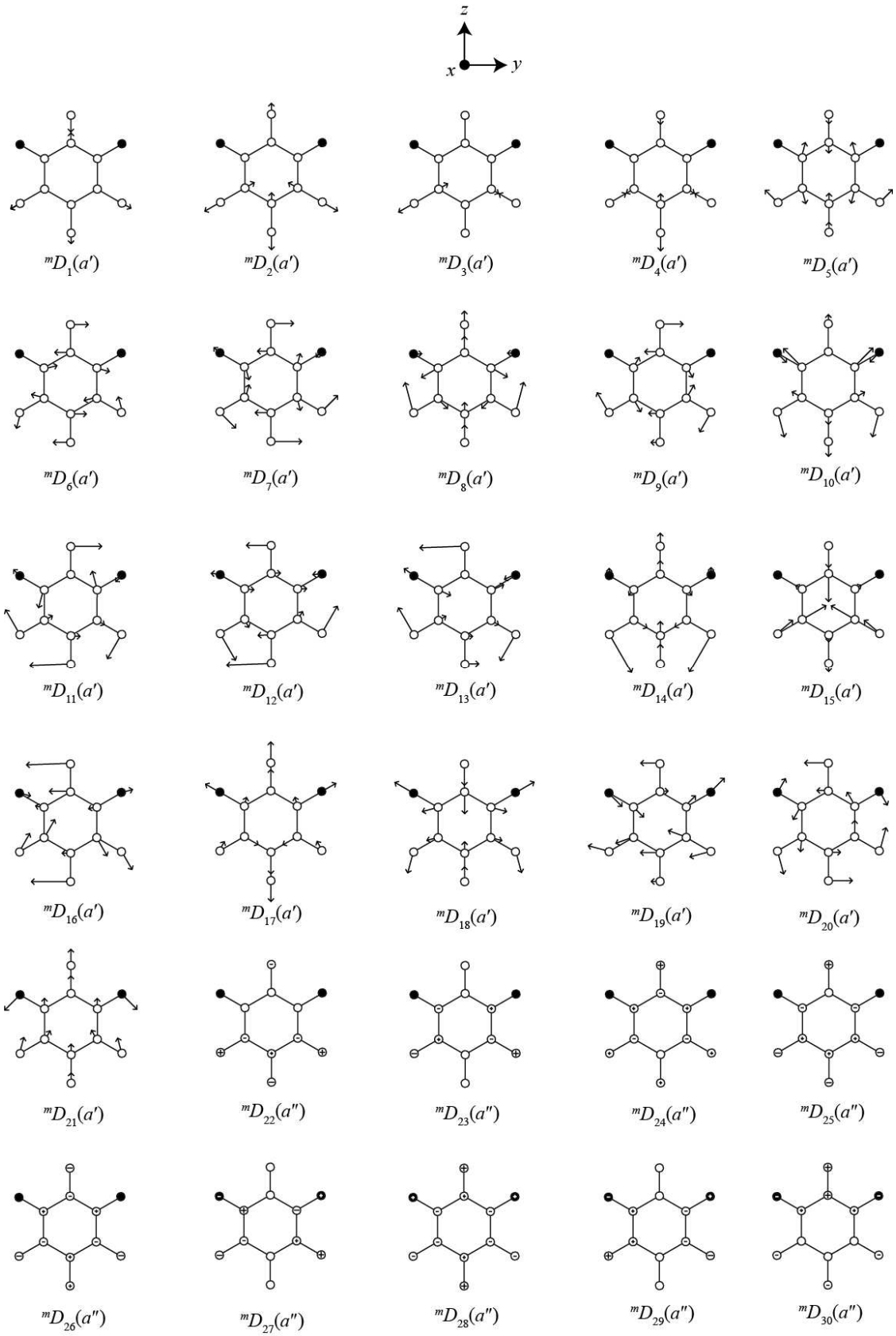
z
x
y
$^{m}D_{1}(a')$
$^{m}D_{2}(a')$
$^{m}D_{3}(a')$
$^{m}D_{4}(a')$
$^{m}D_{5}(a')$
$^{m}D_{6}(a')$
$^{m}D_{7}(a')$
$^{m}D_{8}(a')$
$^{m}D_{9}(a')$
$^{m}D_{10}(a')$
$^{m}D_{11}(a')$
$^{m}D_{12}(a')$
$^{m}D_{13}(a')$
$^{m}D_{14}(a')$
$^{m}D_{15}(a')$
$^{m}D_{16}(a')$
$^{m}D_{17}(a')$
$^{m}D_{18}(a')$
$^{m}D_{19}(a')$
$^{m}D_{20}(a')$
$^{m}D_{21}(a')$
$^{m}D_{22}(a'')$
$^{m}D_{23}(a'')$
$^{m}D_{24}(a'')$
$^{m}D_{25}(a'')$
$^{m}D_{26}(a'')$
$^{m}D_{27}(a'')$
$^{m}D_{28}(a'')$
$^{m}D_{29}(a'')$
$^{m}D_{30}(a'')$

Figure 10

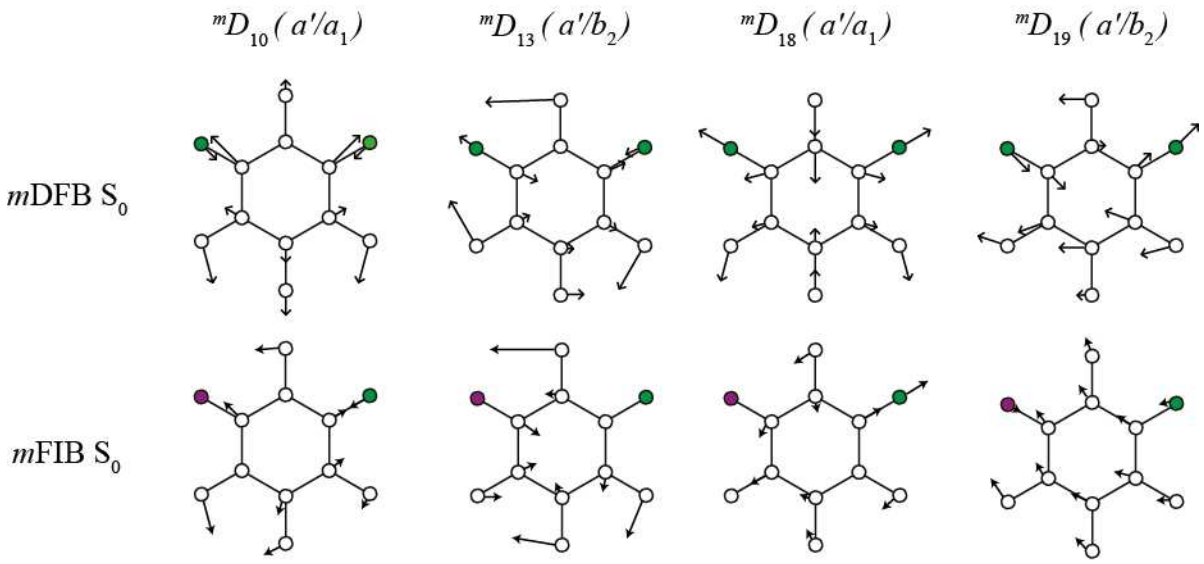

References

[1] E. B. Wilson, Jr, Phys. Rev. 45 (1934) 706.

[3] G. Varsányi, *Assignments of the Vibrational Spectra of Seven Hundred Benzene Derivatives* (Wiley, New York, 1974).

[3] R. S. Mulliken, J. Chem. Phys. 23 (1955) 1997.

[4] G. Herzberg, *Molecular Spectra and Molecular Structure II: Infrared and Raman Spectra of Polyatomic Molecules* (Krieger, Malabar, 1991), p.272.

[5] A. M. Gardner and T. G. Wright. J. Chem. Phys. 135 (2011) 114305.

[6] A. Andrejeva, A. M. Gardner, W. D. Tuttle, and T. G. Wright, J. Molec. Spectrosc. 321 (2016) 28.

[7] W. D. Tuttle, A. M. Gardner, A. Andrejeva, D. J. Kemp, J. C. A. Wakefield and T. G. Wright, J. Molec. Spectrosc. 344 (2018) 46.

[8] J. P. Harris, A. Andrejeva, W. D. Tuttle, I. Pugliesi, C. Schriever, and T. G. Wright, J. Chem. Phys. 141 (2014) 244315.

[9] A. Andrejeva, W. D. Tuttle, J. P. Harris, and T. G. Wright, J. Chem. Phys. 143 (2015) 104312.

[10] A. Andrejeva, W. D. Tuttle, J. P. Harris, and T. G. Wright, J. Chem. Phys. 143 (2015) 244320.

[11] A. M. Gardner, A. M. Green, V M. Tamé-Reyes, V. H. K. Wilton and T. G. Wright
J. Chem. Phys. 138 (2013) 134303.

[12] A. M. Gardner, A. M. Green, V. M. Tamé-Reyes, K. L. Reid, J. A. Davies, V. H. K. Parkes and T. G. Wright J. Chem. Phys. 140 (2014) 114038.

[13] J. R. Gascooke and W. D. Lawrance, J. Chem. Phys., 138 (2013) 134302.

[14] A. M Gardner, W. D. Tuttle, L. Whalley, A. Claydon, J. H. Carter, and T G. Wright, J. Chem. Phys. 145 (2016) 124307.

[15] W. D. Tuttle, A. M. Gardner, L. E. Whalley and T. G. Wright, J. Chem. Phys. 146 (2017) 244310.

[16] W. D. Tuttle, A. M Gardner, K. B. O'Regan, W. Malewicz, and T. G. Wright, J. Chem. Phys. 146 (2017) 124309.

[17] A. M. Gardner, W. D. Tuttle, P. Groner, and T. G. Wright, J. Chem. Phys. 146 (2017) 124308.

[18] W. D. Tuttle, A. M. Gardner, and T. G. Wright, Chem. Phys. Lett. 684 (2017) 339.

[19] *Gaussian 09*, Revision E.01, M. J. Frisch, G. W. Trucks, H. B. Schlegel, G. E. Scuseria, M. A. Robb, J. R. Cheeseman, G. Scalmani, V. Barone, B. Mennucci, G. A. Petersson, H. Nakatsuji, M. Caricato, X. Li, H. P. Hratchian, A. F. Izmaylov, J. Bloino, G. Zheng, J. L. Sonnenberg, M. Hada, M. Ehara, K. Toyota, R. Fukuda, J. Hasegawa, M. Ishida, T. Nakajima, Y. Honda, O. Kitao, H. Nakai, T. Vreven, J. A. Montgomery, Jr., J. E. Peralta, F. Ogliaro, M. Bearpark, J. J. Heyd, E. Brothers, K. N. Kudin, V. N. Staroverov, R. Kobayashi, J. Normand, K. Raghavachari, A. Rendell, J. C. Burant, S. S. Iyengar, J. Tomasi, M. Cossi, N. Rega, J. M. Millam, M. Klene, J. E. Knox, J. B. Cross, V. Bakken, C. Adamo, J. Jaramillo, R. Gomperts, R. E. Stratmann, O. Yazyev, A. J. Austin, R. Cammi, C. Pomelli, J. W. Ochterski, R. L. Martin, K. Morokuma, V. G. Zakrzewski, G. A. Voth, P. Salvador, J. J. Dannenberg, S. Dapprich, A. D. Daniels, Ö. Farkas, J. B. Foresman, J. V. Ortiz, J. Cioslowski, and D. J. Fox, Gaussian, Inc., Wallingford CT, 2009.

[20] I. Pugliesi and K. Muller-Dethlefs, J. Phys. Chem. A 110 (2006) 4657. A free download of the software can be found at http://www.fclab2.net

[21] J. H. S. Green, Spectrochim. Acta. 26A (1970) 1523.

[22] J. H. S. Green, W. Kynaston and H. M. Paisley, J. Chem. Soc. 473 (1963).

[23] E. E. Ferguson, R. L. Collins, J. R. Nielsen and D. C. Smith, J. Chem. Phys. 21, 1470 (1953)

[24] G. A. Crowder amd D. W. Scott, J. Chem. Phys. 21, 1470 (1953)

[25] E. Herz, Monatsch. 74, 160 (1942)

[26] J. R. Scherer and J. C. Evans, Spectrochim. Acta 19, 1754 (1963).

[27] K. W. F Kohlrausch and G. P. Ypsilanti, Monatsch. 66, 285 (1935)

[28] P. A. Graham and S. H. Kable, J. Chem. Phys. 103, 15 (1995).

[29] H. W. Wilson, Spectrochim. Acta 30A (1974) 2141.

[30] S. A. Kudchadker, A. P. Kudchadker, R. C. Wilhoit and B. J. Zwolinski, Thermochim. Acta 30 (1979) 319.

[31] A. Hidalogo and C. Otero. Spectrochim. Acta 16 (1960) 528.

[32] K. S. Pitzer and D. W. Scott, J. Am. Chem. Soc. 65, 803 (1943).

[33] J.K. Wilmshurst and H. S. Bernstein, Can. J. Chem. 35, 911 (1957)

[34] C. Garrigou-Lagrange, M. Chehata and J. Lascombe, J. Chim. Phys. 63, 552 (1966).

[35] J. I. Selco and P. G. Carrick. J. Mol. Spec. 173, 262 (1995)

[36] K. W. F Kohlrausch and A. Pongratz, Monatsch. 65, 199 (1935)

[37] J. H. S. Green, D. J. Harrison and W. Kynaston. Spectrochim. Acta 27A (1971) 2199.